



OPEN

Antiviral activities of plant-derived indole and β -carboline alkaloids against human and avian influenza viruses

Akram Hegazy^{1,6}, Sara H. Mahmoud^{2,6}, Yaseen A. M. M. Elshaier³, Noura M. Abo Shama², Nasr Fawzy Nasr¹, M. A. Ali¹, Assem Mohamed El-Shazly^{4,5}, Islam Mostafa⁴✉ & Ahmed Mostafa²✉

The persistent evolution of drug-resistant influenza strains represents a global concern. The innovation of new treatment approaches through drug screening strategies and investigating the antiviral potential of bioactive natural-based chemicals may address the issue. Herein, we screened the anti-influenza efficacy of some biologically active indole and β -carboline (β C) indole alkaloids against two different influenza A viruses (IAV) with varied host range ranges; seasonal influenza A/Egypt/NRC098/2019(H1N1) and avian influenza A/chicken/Egypt/N12640A/2016(H5N1). All compounds were first assessed for their half-maximal cytotoxic concentration (CC_{50}) in MDCK cells and half-maximal inhibitory concentrations (IC_{50}) against influenza A/H5N1. Intriguingly, Strychnine sulfate, Harmalol, Harmane, and Harmaline showed robust anti-H5N1 activities with IC_{50} values of 11.85, 0.02, 0.023, and 3.42 μ g/ml, respectively, as compared to zanamivir and amantadine as control drugs (IC_{50} = 0.079 μ g/ml and 17.59 μ g/ml, respectively). The efficacy of the predefined phytochemicals was further confirmed against influenza A/H1N1 and they displayed potent anti-H1N1 activities compared to reference drugs. Based on SI values, the highly promising compounds were then evaluated for antiviral efficacy through plaque reduction assay and consistently they revealed high viral inhibition percentages at non-toxic concentrations. By studying the modes of antiviral action, Harmane and Harmalol could suppress viral infection via interfering mainly with the viral replication of the influenza A/H5N1 virus, whilst Harmaline exhibited a viricidal effect against the influenza A/H5N1 virus. Whereas, Strychnine sulfate elucidated its anti-influenza potency by interfering with viral adsorption into MDCK cells. Consistently, chemoinformatic studies showed that all studied phytochemicals illustrated HB formations with essential peptide cleft through the NH of indole moiety. Among active alkaloids, harmalol displayed the best lipophilicity metrics including ligand efficiency (LE) and ligand lipophilic efficiency (LLE) for both viruses. Compounds geometry and their ability to participate in HB formation are very crucial.

Abbreviations

IC_{50}	Half maximal inhibitory concentration
CC_{50}	Half maximal cytotoxic concentration
SI	Selectivity Index
MDCK	Madin Darby Canine Kidney
HPAIV	Highly pathogenic avian influenza virus
SARS-CoV-2	Severe acute respiratory syndrome coronavirus 2
LE	Ligand efficiency

¹Department of Agricultural Microbiology, Faculty of Agriculture, Cairo University, Giza District 12613, Giza, Egypt. ²Center of Scientific Excellence for Influenza Viruses, National Research Centre, Giza 12622, Egypt. ³Department of Organic and Medicinal Chemistry, Faculty of Pharmacy, University of Sadat City, Sadat City 32897, Menoufia, Egypt. ⁴Department of Pharmacognosy, Faculty of Pharmacy, Zagazig University, Zagazig 44519, Sharkia, Egypt. ⁵Faculty of Pharmacy, El Saleheya El Gadida University, El Saleheya El Gadida 44813, Sharkia, Egypt. ⁶These authors contributed equally: Akram Hegazy and Sara H. Mahmoud. ✉email: i_m_elbaz@zu.edu.eg; ah.mostafa@nrc.sci.eg

LLE	Ligand lipophilic efficiency
NHA	Non-hydrogen atom
SAR	Structure–activity relationship

Over the last century, the pandemic consequences of influenza A viruses (IAV) are more hazardous and frequent, even when compared with the morbidity and mortality rates of the current devastating global pandemic of COVID-19^{1,2}.

The Influenza viruses are belonging to the Orthomyxoviridae family and are classified into 4 genera: influenza A (IAV), influenza B (IBV), influenza C (ICV), and influenza D (IDV) viruses. All reported occasional influenza pandemics and seasonal epidemics are caused mainly by IAV infections^{1,3}. The evolution of pandemic IAV variants occurs commonly via the genetic exchange between viral RNA segments of different subtypes of IAVs in a genomic phenomenon called “antigenic shift or reassortment”. Whereas, the evolution of endemic IAV variants occurs via a continuous change in the viral RNA genome during viral replication “antigenic drift” in different hosts^{1,4}.

The innovation of antivirals has long paved the way for treating influenza in developing and developed countries. However, the future efficacy of the commercially available antivirals is somewhat suspicious because viruses are developing resistance in an inevitable way to the already established antiviral drugs. Plants are still the best choice for extracting and isolating naturally-based antiviral agents⁵.

Alkaloids are belonging to a major chemical group that is found in microbes, plants, and animals⁶. These small cyclic nitrogenous compounds are alkaline in nature, hence the name, and they are found in 20% of plants⁷. They are categorized into indole, quinoline, isoquinoline, tropane, steroidal, pyridine, and pyrrolizidine based on their molecular structure⁸. Indole alkaloids class are those alkaloids with an organic structure consisting of a pyrrole linked to a benzene ring. Such compounds are produced from plants as secondary metabolites, and they exhibited antiviral activities against a wide variety of viruses such as IAV⁹, hepatitis C virus (HCV)¹⁰, human immunodeficiency virus-1 (HIV-1)¹¹, dengue virus (DENV)¹², zika virus (ZIKV) and chikungunya virus (CHIKV)¹³ and may play a key role in combating the newly emerged coronavirus; severe acute respiratory syndrome coronavirus-2 (SARS-CoV-2)^{14–16}. The aromatic compounds: β -carbolines (naturally and/or synthetically indole alkaloid derivatives) possess numerous biological activities including antiviral activities against different emerging and reemerging viruses such as herpes simplex virus-1 (HSV-2), DENV-2, and enterovirus-71 (EV-71), HIV and Poliovirus (PV)^{17–20}. The β -carbolines are common in *Peganum harmala*, this plant is common in Egypt. In folk medicine, it is used as an analgesic, antiseptic, and emmenagogue and in the treatment of asthma, colic, jaundice, and lumbago²¹.

Herein, we investigated the antiviral potential of some purified naturally derived indole and β -carboline indole alkaloids against avian and human influenza A/H5N1 and A/H1N1viruses, respectively. The virtual mode of action for the biologically active alkaloids was also provided.

Materials and methods

Cell lines and viruses. Madin Darby Canine Kidney (MDCK) cells were kindly obtained from the cell culture collections of the Centre of Scientific Excellence for Influenza Viruses at Egyptian National Research Centre and were grown in Dulbecco's Modified Eagle's Medium (DMEM) (DMEM; BioWhittaker, Walkersville, MD, USA) supplemented with fetal bovine serum (FBS) (10%) (Gibco-BRL; New York, USA) and penicillin/streptomycin (pen/strep) antibiotic/antimycotic mixture (2%) (GIBCO-BRL; New York, USA) and cultured under the optimum growth conditions; 37 °C/ 5% CO₂/humidified conditions.

Both the HPAIV A/chicken/Egypt/N12640A/2016(H5N1)²² and the seasonal influenza A/Egypt/NRC098/2019(H1N1) (GISAID ID: EPI_ISL_12995118) were provided by the Egyptian Center of Scientific Excellence for Influenza Viruses, National Research Center, Egypt and inoculated either in MDCK cells and/or specific pathogen-free (SPF) embryonated chicken eggs to propagate them as described earlier^{22,23}.

Compounds under investigation. The tested compounds used in our investigation are listed, in detail (Table 1). Strychnine sulfate, reserpine, brucine, eserine, harmine, and norharmine were purchased from Sigma-Aldrich (Sigma-Aldrich, Germany). Harmine, harmaline, and harmalol were purchased from the Molekula group (Molekula, Germany). Methyl ergometrine was obtained from Novartis (Al-Amiria District, Cairo). Their documented biological activities/chemical nucleus served as the basis for their selection to be examined for their antiviral potential against IAVs. The molecular structures of the studied compounds are shown (Fig. 1).

Virus titration. *Median tissue culture infectious dose (TCID₅₀) method.* To determine the viral dilutions that can infect 50% of the MDCK cell line, we conducted the TCID₅₀ method according to Reed and Muench method (1938)⁴¹ method. Briefly, ten-fold serial viral dilutions, in triplicates, were allowed to infect MDCK cell monolayers and incubated at 37 °C in a humidified 5% CO₂ incubator for 72 h.

After incubation, plates were decontaminated and cells were fixed using a 10% paraformaldehyde solution. An aliquot of 100 μ l crystal violet stain (0.1% in methanol) was added to each well and allowed to incubate at room temperature for 10 min. Plates were next thoroughly washed with water to remove excess staining material and dried overnight. Once dried, plates were assessed for cytopathic effect (CPE) in each column. The final titer was calculated using the Reed–Muench Method⁴¹.

Plaque infectivity assay (PIA). To define the countable viral titer of IAVs and define their stock titers as plaque-forming units (PFU)/ml, PIA was performed as previously described⁴² with minor modifications. Briefly, the 80–90% confluent MDCK cell monolayers (precultured at a density of 1.2×10^6 cells/well in 6 well plate) were

Compound	Class	Biological activities	Viruses	Citation
Strychnine Sulfate	Indole Alkaloids	Antitumor	N/A	24
Reserpine	Indole Alkaloids	Anti-inflammatory, antihypertensive, and antiviral activities	SARS-CoV	15,25,26
Brucine	Indole Alkaloids	Anticarcinogenic, neurotoxic, anti-inflammatory, and analgesic	N/A	27–29
Methyl ergometrine	Indole Alkaloids	Antihemorrhagic	N/A	30
Eserine	Indole Alkaloids	Anticholinesterase and antiviral	SARS-CoV-2	14,31
Harmine	β -carboline Indole Alkaloids	Anticarcinogenic, antiviral antifungal, antimicrobial, antiparasitoid, and antioxidant	HSV-2, DENV-2, and EV-71	17–20
Harmalol	β -carboline Indole Alkaloids	Anticarcinogenic and antifungal	N/A	32,33
Harmame	β -carboline Indole Alkaloids	Antianxiety, antidepressant, antidiabetic, antioxidant, antiparasitic and antiviral	HSV-1 & HSV-2	34–36
Harmaline	β -carboline Indole Alkaloids	Antioxidant and anti-tumor	N/A	37,38
Norharmane	β -carboline Indole Alkaloids	Anticancer and antibacterial	N/A	39,40

Table 1. The tested indole alkaloid and β -carboline indole alkaloid compounds.

washed with 1X phosphate buffer saline (1xPBS) and infected with 100 μ l/well of the ten-fold serial dilutions for each virus in 1xDMEM (supplemented with 4% bovine serum albumin (BSA) (Gibco-BRL; New York, USA), 2% pen/strep mixture and 1 mg/mL of L-1-tosyl- amido-2-phenylethyl chloromethyl ketone (TPCK)-treated trypsin). The plates were incubated for 1 h in a humidified condition with 5% CO₂ and 37 °C to allow for viral adsorption. The plates were gently shaken during the incubation period at intervals of 15 min. The inocula were then removed and the plates were overlaid with 2% agarose/2xDMEM overlay, then the plates were incubated for 72 h at 37 °C with 5% CO₂ in a humidified condition. The plates underwent fixation with 10% formaldehyde and were further stained with 0.1% crystal violet (CV) solution to visualize the viral plaques. The following formula was used to determine the viral titer for each virus:

$$\text{Plaque forming unit } \frac{\text{PFU}}{\text{ml}} = \text{Number of plaques} * \text{Reciprocal of virus dilution} * \text{Dilution factor (to 1 ml)}$$

Cytotoxicity and antiviral assays. The crystal violet assay was employed as previously described to determine the half maximum cytotoxic concentration 50 (CC₅₀) on MDCK cells and the half maximal inhibitory concentrations 50 (IC₅₀) for each compound^{43–45}. Briefly, MDCK cells were cultivated into cell culture plates (100 μ l/well at a density of 3 \times 10⁵ cells/mL) and incubated for 24 h under the optimal previously described growth conditions. Next, the plates were washed with sterile 1xPBS, and successive ten-fold serial dilutions of the investigated natural-based compounds were added to the cultured wells in triplicate including untreated cell control wells. The plates were then incubated at 37 °C / 5% CO₂ in humidified conditions for 3 days to assess the CC₅₀ for each compound. After the incubation period, the cell monolayers were fixed with 10% formaldehyde and then stained with 0.1% crystal violet. The crystal violet stain in dried plates was then dissolved by adding absolute methanol. The optical density (OD) was measured using an ELISA plate reader at a wavelength of 570 nm.

The IC₅₀ was performed as previously described⁴⁴. In 96-well tissue culture plates, MDCK cells were distributed in each well as described previously and incubated overnight at a humidified 37 °C incubator under 5% CO₂ condition. The cell monolayers were then washed once with 1 \times PBS and subjected to virus adsorption (100 TCID₅₀/ml) for 1 h at room temperature (RT). The cell monolayers were further overlaid with 100 μ l of 1xDMEM containing varying safe concentrations of the test compounds, including untreated cell control wells and virus-infected untreated cells as a virus control for normalization. Following incubation at 37 °C in a 5% CO₂ incubator for 72 h, the cells were fixed with 100 μ l of 4% paraformaldehyde for 20 min and stained with 0.1% crystal violet in distilled water for 15 min at RT. The crystal violet dye was then dissolved using 100 μ l absolute methanol per well and the optical density of the color is measured at 570 nm using Anthos Zenyth 200rt plate reader (Anthos Labtec Instruments, Heerhugowaard, Netherlands). The IC₅₀ of the compound is that required to reduce the virus-induced cytopathic effect (CPE) by 50%, relative to the virus control.

Plaque reduction assay (PRA). To further verify the anti-influenza potential of the most promising candidates based on their IC₅₀ values, the PRA was conducted according to Mostafa and coworkers⁴⁴ with minor modifications. Briefly, the MDCK cells were cultured in 6 well plate at a density of 1.2 \times 10⁶ cells/well under

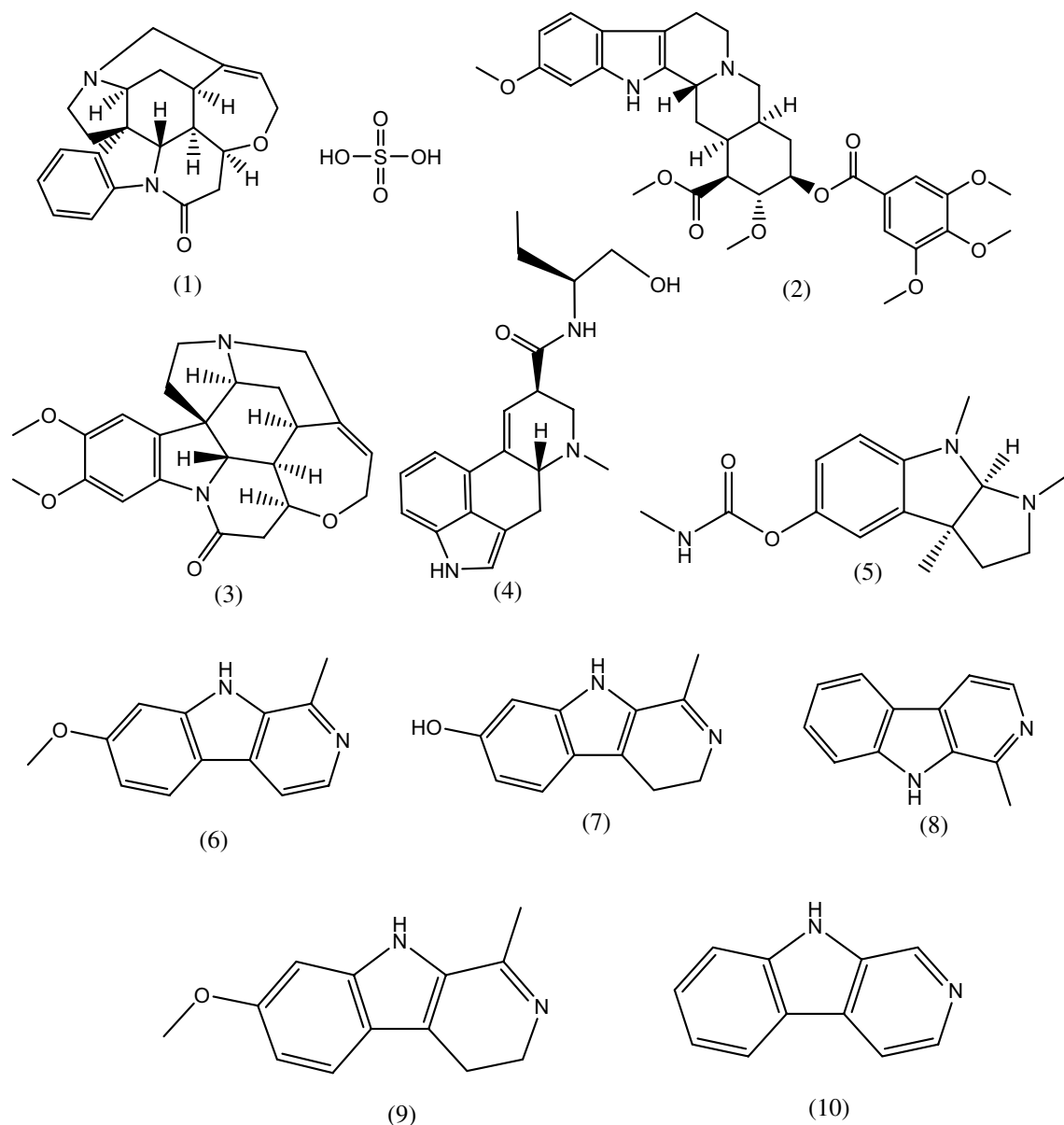


Figure 1. The molecular structures of the studied compounds. (1) Strychnine sulfate, (2) Reserpine, (3) Brucine, (4) Methyl ergometrine, (5) Eserine, (6) Harmine, (7) Harmalol, (8) Harmane, (9) Harmaline, (10) Norharmane.

the optimum growth conditions; 37 °C in humidified 5% CO₂ conditions. The non-toxic concentrations of each compound were mixed with countable virus dilution (A/H1N1 or A/H5N1) in 1xDMEM supplemented with 4% BSA, 2% pen/strep mixture, and TPCK-treated trypsin and incubated at room temperature for 1 h. To allow viral adsorption, the mixture was added to the MDCK cell monolayer (80–90% confluency) under optimal growth conditions and incubated for 1 h at 37 °C in a humidified 5% CO₂ incubator. The inocula were then aspirated and 2% agarose/2 × DMEM overlays were added. The plates were incubated at 37 °C in a humidified 5% CO₂ incubator for 72 h. The cell monolayers in plates were then fixed with 10% formaldehyde and further stained with 0.1% crystal violet (CV) solution to visualize the viral plaques. The percent of viral reduction was calculated using the following equation:

$$\text{Plaque reduction (\%)} = \frac{\text{Count of untreated virus (control)} - \text{Count of treated virus}}{\text{Count of untreated virus (control)}} \times 100$$

Possible stage(s) of antiviral action. To define the possible stage(s) of antiviral action for each anti-influenza candidate hitting high selectivity index, the plaque reduction assay⁴⁶ was carried out with some modifications to discover the critical step at which the tested compound work against the influenza A/H5N1 virus. According to Mostafa and coworkers⁴⁴, the compound exerts its antiviral effect using the following mechanisms:

(1) hindering the viral multiplication inside the host cell, (2) hindering the viral adsorption onto the host cell, or (3) direct viricidal effect against the virus (a cell-free mechanism).

Viral replication interference. The viral dilutions of influenza A/H5N1 virus were allowed to infect the MDCK cells that were previously cultured at a density of 1.2×10^6 cells/well in 6 well plate for 24 h under optimal conditions. Each plate contains cell and virus control wells to ensure the validity of the assay and to calculate the percent of viral inhibition following treatment, respectively. The plates were then incubated at 37 °C in a humidified 5% CO₂ incubator for 1 h. The cell monolayers were then washed with 1xPBS to remove the residues of the infection process. Subsequently, the different predetermined non-cytotoxic concentrations of each compound were applied, and the plates underwent a second incubation period at 37 °C in a humidified 5% CO₂ incubator for 1 h. Another washing step was applied and the 2% agarose overlays were added then the plates were incubated at 37 °C in a humidified 5% CO₂ incubator for 72 h. The cell monolayers were then fixed and stained, visualized using 0.1% crystal violet solution as described previously in the plaque infectivity assay.

Viral adsorption interference. A range of non-cytotoxic concentrations was applied to the precultured MDCK cells in 6 well plates (1.2×10^6 cells/well). Each plate contains cell and virus control wells to ensure the validity of the assay and to calculate the percent of viral inhibition following treatment, respectively. The plates were then incubated in the refrigerator (4 °C) for 1 h to allow chemical adsorption onto cell receptors without active penetration. The plates were then washed with 1xPBS to remove the residual compounds. Subsequently, the countable viral dilution of influenza A/H5N1 virus was applied to allow viral adsorption/infection and another incubation period was employed at 37 °C in a humidified 5% CO₂ incubator for 1 h. The cell monolayers were then washed with 1xPBS to remove the residual virus and overlaid with 2% Agarose/2xDMEM overlay and incubated at 37 °C in a humidified 5% CO₂ incubator for 72 h. The cell monolayers were then fixed and stained, visualized using 0.1% crystal violet solution as described previously in the plaque infectivity assay.

Viricidal effect. A simple plaque reduction assay was performed where effective concentrations of the compounds were mixed with concentrated influenza A/H5N1 virus (3–4 folds higher than the countable virus dilution). The virus/compound mixture was then incubated at room temperature for 1 h. Subsequently, ten-fold serial dilutions of the virus/compound mixture (3 or 4 times) were performed to reach a countable viral titer. The mixture dilution with countable viral titer was then applied to the MDCK monolayers (1.2×10^6 cells/well) including cell and virus control wells. The plates were then incubated at 37 °C in a humidified 5% CO₂ incubator for 1 h. To remove the remains of the mixture, cell monolayers were washed with 1xPBS and overlaid with 2% agarose/2xDMEM, and incubated at 37 °C in a humidified 5% CO₂ incubator for 72 h. The cell monolayers were then fixed and stained, visualized using 0.1% crystal violet solution as described previously in the plaque infectivity assay.

Cheminformatics studies. *Molecular docking.* The X-ray crystal structure coordinate of (PDB ID: 6hp0⁴⁶ and PDB: ID:6bkk^{47,48}) were retrieved from PDB with their co-crystallized bound ligands. The study is represented in detail against PDB ID: 6hp0). The docking study was performed using openEye scientific software version 2.2.5 (SantaFe, NM (USA), <http://www.eyesopen.com>), academic license (The Laboratory of Yaseen A. M. Mohamed Elshaier. A virtual library of the synthesized compounds was used, and their energies were minimized using the MMFF94 force field, followed by the generation of multi-conformers using the OMEGA application. The library was compiled in one file by Omega. The target proteins were retrieved from PDB and the created receptor was operated by the OeDocking application. Both the ligand input file and the receptor input file were subjected to FRED to implement the molecular docking study. Multiple scoring functions were engaged to predict the energy profile of the ligand-receptor complex. The vida application was used as a visualization method. The dimension for created box of receptors were as follow: Box volume: 5544 Å, dimension 21.00 Å × 18.00 Å × 14.67 Å.

Physicochemical parameter and lipophilicity calculations. Compound parameters, including clogP, were calculated by using the free-access website <http://www.eyesopen.com>.

Biosafety and biosecurity. All experiments with infectious viruses were performed according to Egyptian regulations for the propagation of influenza viruses. The low pathogenic seasonal IAV and the highly pathogenic AIV were handled in biosafety level 2 (BSL-2) and 3 (BSL-3) conditions in two separate laboratories, respectively, approved for such use by the local authorities.

Results

Cytotoxicity and viral inhibitory activity of the screened alkaloid compounds. The assessment of cytotoxicity of the tested indole and β-carboline indole alkaloids (Table 1) is a critical step for further evaluating their anti-influenza potential activity. The cytotoxicity of the screened alkaloid compounds was evaluated in MDCK cells (Fig. 2) and they all showed a wide range of safe, non-toxic concentrations (from 1 ng/ml to 10 mg/ml).

Thereafter, the anti-influenza potential activity of each compound was investigated at non-cytotoxic concentrations against HPAIV A/H5N1, compared to the reference anti-influenza neuraminidase inhibitor zanamivir and the M2-proton channel blocker amantadine. Remarkably, the indole alkaloid; Strychnine sulfate demonstrated a significant effect with an IC₅₀ value of 11.851 µg/ml, and in the same context, the β-carboline indole

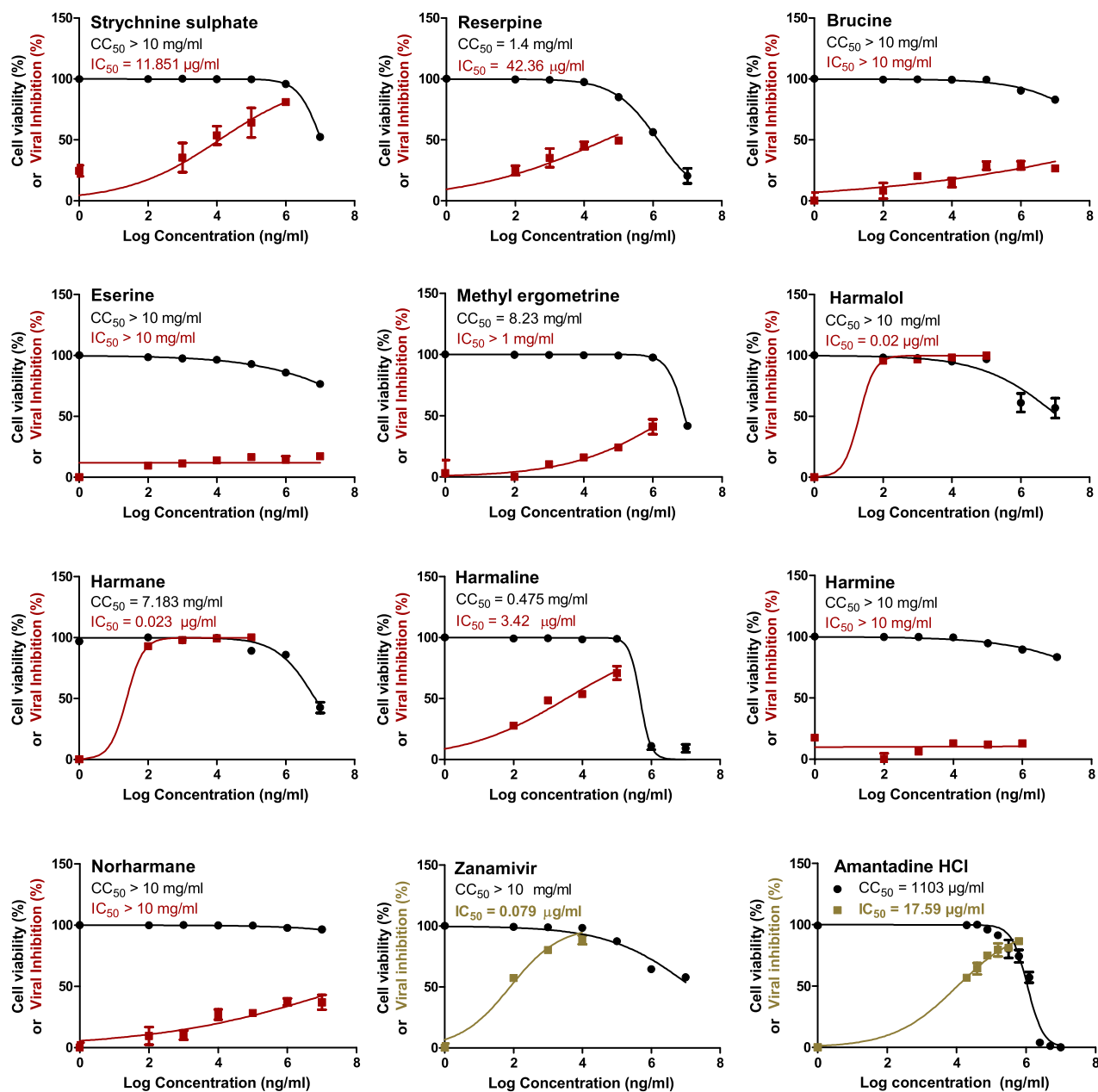


Figure 2. The cytotoxic and anti-H5N1 effects of the screened compounds in the MDCK cell line. By employing the crystal violet assay and nonlinear regression analysis of the GraphPad Prism program (version 5.01) by plotting log inhibitor versus normalized response (variable slope), the CC₅₀ and IC₅₀ of the examined indole and β-carboline indole alkaloids were determined.

alkaloids; Harmalol, Harmane and Harmaline exhibited strong anti-influenza effects with the IC₅₀ values of 0.02, 0.023 and 3.42 μg/ml, respectively, with unexpected very high selectivity indices (SIs) (Fig. 2 and Table 2). On the same hand, as compared to the drug controls, Reserpine elucidated a moderate anti-influenza activity with an IC₅₀ value of 42.36 μg/ml. Unlikely, Brucine, Eserine, Methyl ergometrine, Harmine, and Norharmane proved poor or no antiviral potential activity against the avian influenza A/H5N1 virus.

To confirm that the obtained anti-influenza activities of Strychnine sulfate, Harmalol, Harmane, and Harmaline are not strain-specific, their anti-influenza activity was further investigated against human influenza A/H1N1 virus and compared to the anti-influenza zanamivir and amantadine drug controls. Consistently, Strychnine sulfate, Harmalol, Harmane, and Harmaline exerted potent anti-influenza activity against influenza A/H1N1 virus with IC₅₀ values of 0.06, 0.035, 0.033, and 0.056 μg/ml respectively (Fig. 3).

Viral plaque reduction of the investigated compounds. The screened alkaloids with promising anti-influenza activities as indicated with low IC₅₀ values and high SI values were subjected further to plaque reduction assay to validate their anti-influenza efficacy against HPAIV A/H5N1 and seasonal influenza A/H1N1 viruses. The tested indole and β-carboline indole alkaloids demonstrated remarkable capacity to elicit viral sup-

Phytochemical compound	Chemical classification	IAV subtype	CC ₅₀ (mg/ml)	IC ₅₀ (μg/ml)	Selectivity index (SI)	
Strychnine Sulfate	Indole Alkaloids	H5N1	> 10	11.851	> 843	
		H1N1		0.06	> 1.67*10 ⁵	
Reserpine		H5N1	1.4	42.36	> 33	
		H1N1		ND	N/A	
Brucine		H5N1	> 10	> 10,000	N/A	
		H1N1		ND	N/A	
Eserine		H5N1	> 10	> 10,000	N/A	
		H1N1		ND	N/A	
Ergometrine		H5N1	8.23	> 1000	N/A	
		H1N1		ND	N/A	
Harmalol		β-Carboline Indole Alkaloids	H5N1	> 10	0.02	> 5*10 ⁵
			H1N1		0.035	> 2.8*10 ⁵
Harmame	H5N1		7.183	0.023	> 3.12*10 ⁵	
	H1N1			0.033	> 2.17*10 ⁵	
Harmaline	H5N1		0.475	3.42	138	
	H1N1			0.056	8482	
Harmine	H5N1		> 10	> 10,000	N/A	
	H1N1			ND	N/A	
Norharmame	H5N1		> 10	> 10,000	N/A	
	H1N1			N/A	N/A	
Zanamivir	NAI (drug control)		H5N1	> 10	0.079	> 1.26*10 ⁵
			H1N1		0.291	> 3.4*10 ⁴
Amantadine HCl	M2-channel blocker	H5N1	1.103	17.59	62.71	
		H1N1		14.86	74.32	

Table 2. Selectivity indices “SIs” for the tested compounds against avian influenza A/H5N1 and human influenza A/H1N1 virus in the MDCK cell line.

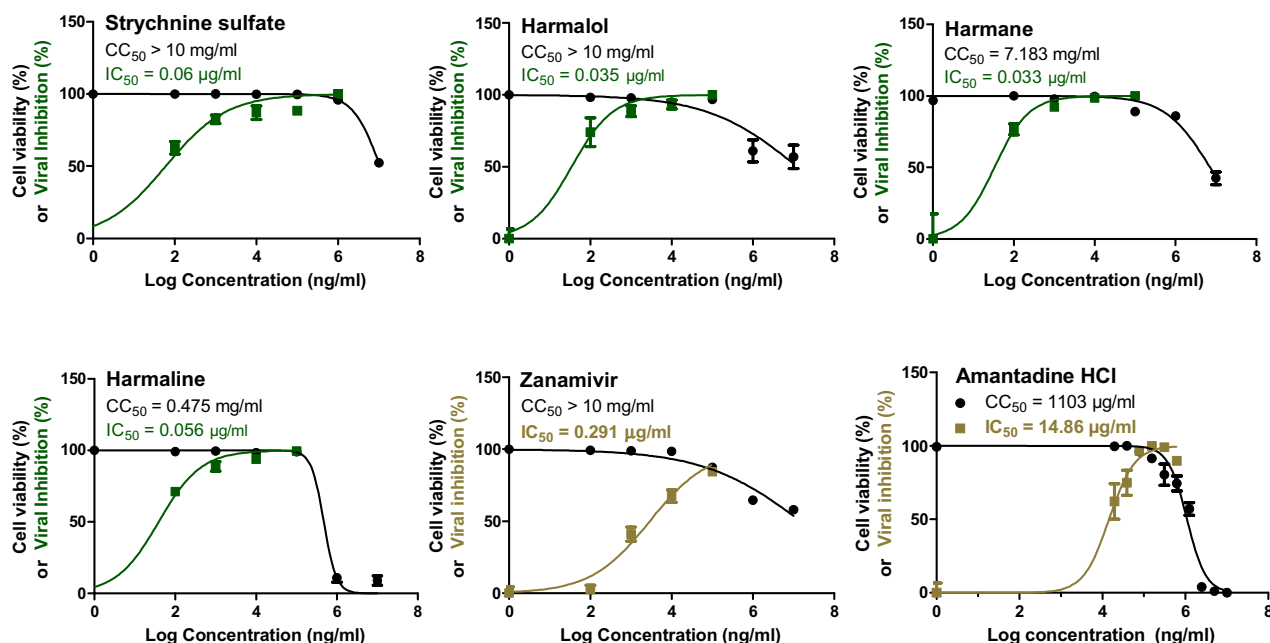


Figure 3. The cytotoxic and anti-H1N1 effects of the screened compounds in the MDCK cell line. By employing the crystal violet assay and nonlinear regression analysis of the GraphPad Prism program (version 5.01) by plotting log inhibitor versus normalized response (variable slope), the CC₅₀ and IC₅₀ of the most promising indole and β-carboline indole alkaloids were computed.

pression at low doses against IAVs that were used in this study (Table 3). These viral inhibitions in plaque forming units were statistically significant among all tested concentrations for each compound when compared to compound-untreated virus control for influenza A/H5N1 (Fig. 4) and A/H1N1 viruses (Fig. 5). These data are consistent with our prior findings.

Stage(s) of antiviral action. To investigate the possible target(s) of the studied compounds with promising anti-influenza activities, we studied three main targets by which the compounds can affect viral infectivity and replication cycle including (1) direct viricidal action, (2) hindering the viral adsorption onto host cell's receptor, and (3) hindering the viral replication machinery. Interestingly, the tested anti-influenza alkaloids could affect the three aforementioned compartments but in varying strengths. Interestingly, Harmalol and Harmane could block influenza A/H5N1 infection via interference with the viral replication compartment. Whereas harmaline exerted a direct cell-free viricidal effect on the viral particle. Finally, Strychnine Sulphate showed the capacity to reduce the viral titer by hindering IAV adsorption to the host cell (MDCK) receptors (Table 4).

Compound	Conc. ($\mu\text{g/ml}$)	Against influenza A/H5N1 virus			Against influenza A/H1N1 virus		
		Viral inhibition (%)			Viral inhibition (%)		
		Mean	SD	N	Mean	SD	N
Harmalol	10	86.42	2.14	3	91.81	1.01	3
	1	73.33	2.31	3	79.63	0.000	3
	0.1	54.67	2.31	3	74.27	1.02	3
Harmane	1000	84.95	1.86	3	84.62	1.01	3
	100	74.44	1.93	3	74.36	2.22	3
	10	65.48	2.06	3	55.13	2.22	3
Harmaline	100	94.25	1.99	3	86.46	1.80	3
	10	87.66	2.14	3	77.78	1.92	3
	1	72.62	2.06	3	66.67	1.86	3
Strychnine sulphate	100	96.30	3.71	3	87.36	1.99	3
	10	83.95	2.14	3	71.61	5.66	3
	1	74.36	2.22	3	65.52	3.45	3

Table 3. Viral reduction percentages following treatment of influenza A/H1N1 and A/H5N1 with a range of non-cytotoxic concentrations of indole and β -carboline indole alkaloids, as measured by plaque reduction assay.

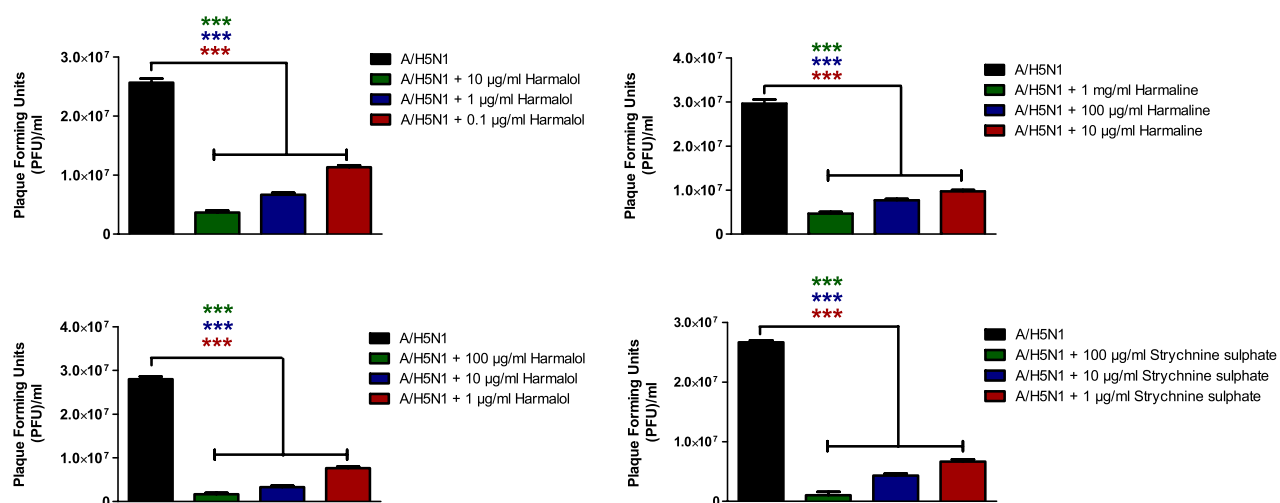


Figure 4. The Plaque forming units (PFU) per ml for compound-untreated influenza A/H5N1 virus control versus multiple concentrations-treated virus. Mean values of results represent the averages from three independent experiments and are presented with standard deviations (SDs) indicated by error bars. Asterisks (***) indicate a significant difference ($p < 0.001$) compared to the compound-untreated influenza A/H5N1 virus control. Statistical analysis was performed using repeated measures ANOVA, followed by Bonferroni post hoc test.

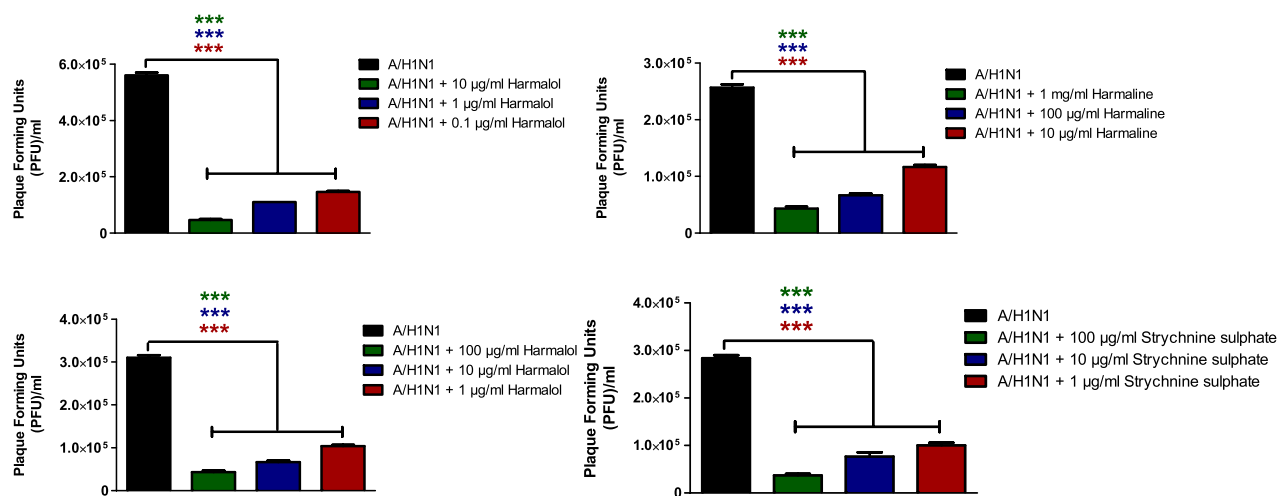


Figure 5. The Plaque forming units (PFU) per ml for compound-untreated influenza A/H1N1 virus control versus multiple concentrations-treated virus. Mean values of results represent the averages from three independent experiments and are presented with standard deviations (SDs) indicated by error bars. Asterisks (***) indicate a significant difference ($p < 0.001$) compared to the compound-untreated influenza A/H1N1 virus control. Statistical analysis was performed using repeated measures ANOVA, followed by Bonferroni post hoc test.

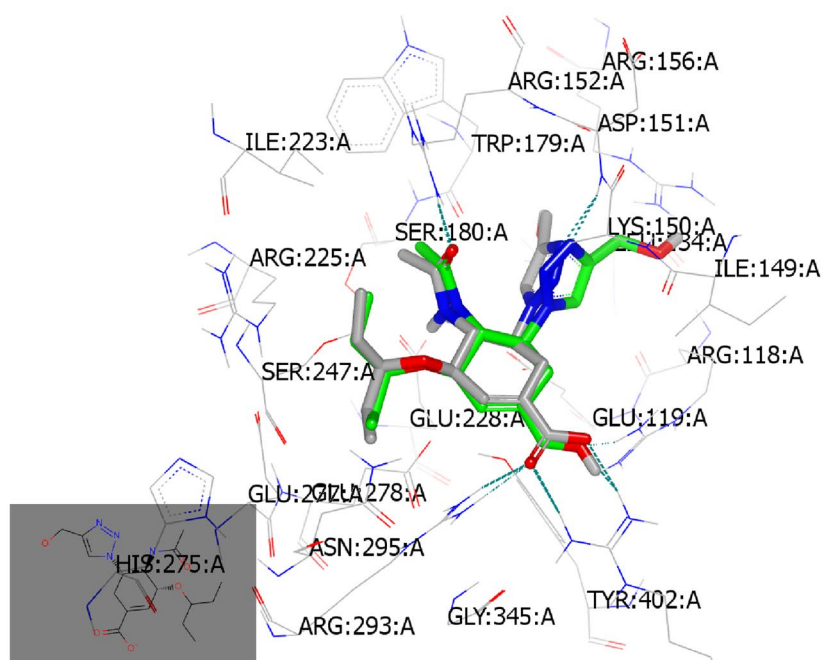
Compound	Concentration (µg/ml)	Mechanism of Action		
		Viral replication (%)	Viricidal (%)	Viral adsorption (%)
Harmalol	0.1	87.5	41.5	60.3
	1	96.9	50.9	74.5
	10	98.7	58	82.1
Harmaline	10	83.3	31.8	43.4
	100	97.5	41.8	48.7
	1000	96.7	82.1	61.4
Harmaline	1	28.3	91	34
	10	40.3	96.7	46.2
	100	48.7	98.6	51.8
Strychnine Sulfate	1	19.4	29.4	90.1
	10	27.3	37	99.5
	100	42	49.2	99

Table 4. The mechanism of antiviral action for the investigated indole and β -carboline indole alkaloids represented as viral inhibition (%) in a concentration-dependent manner.

Chemoinformatic studies. *Molecular docking study with neuraminidase (PDB ID: 6hp0).* Neuraminidase inhibitors hinder the function of the viral neuraminidase protein, preventing virus release from infected host cells to further infect new host cells and thereby freeing the virus to infect other cells in the host organism and subsequently hindering the viral replication cycle^{1,49}. The main structural neuraminidase (NA) inhibitors are cyclohexane scaffold containing lipophilic moiety with modification in the geometry and size of this part⁵⁰. Our active compounds belong to carboline skeleton in which cyclohexene ring fused with indole moiety. These similarities guided us to introduce these compounds as neuraminidase inhibitors. By comparative analysis of the docking mode and pose of our compounds to standard ligands for M2-proton channel blockers and neuraminidase inhibitors, the selected compounds revealed high similarity to the control neuraminidase inhibitors. The current antiviral drugs are likely directed to neuraminidase inhibitor analogues especially with the reported resistance of amantadine to the currently circulating IAV strains including the tested virus strain (Figs. 2 and 3). These evidences directed us to perform the docking against neuraminidase surface glycoprotein.

To validate our docking protocol, the standard ligand was docked by OpenEye software and it was superimposed with its co-crystallized downloaded complex³¹. Both structures displayed the same binding mode and pose with consensus score 10 as the best score. They formed multiple hydrogen bonding (HB) interactions with key amino acids in the receptor active sites especially Arg: 153A, Asp:151A, Arg:293A, Arg:368A, Glu:277A, and Arg:118A. Notably, the standard ligand formed HB interactions with basic amino acids (Fig. 6a).

(a)



(b)

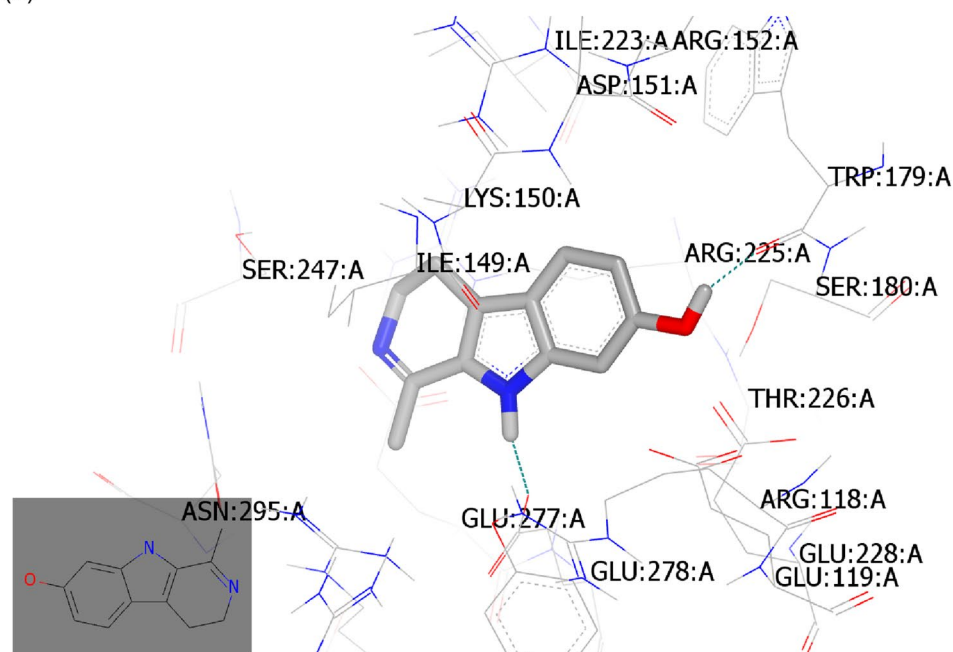


Figure 6. Snapshot of selected compounds represented by Vida application. (a) Standard ligand (grey colour) and its co-crystallized complex (green colour); (b) Harmalol docked with the receptor with the formation of HB (green colour); (c) Harmalol overlay with its methylated isomer, Harmaline; (d) Harmane showed complete overlay with its inactive derivative, Harmine.

Harmalol forms a hydrogen bond (HB) with Trp:179A (as donor) through its OH as acceptor and with Gln:278A through NH, (Fig. 6b) with consensus score 45. The snapshot of harmalol with its methylated isomer, harmaline represented overlay. However, harmaline was not able to form HB interaction with the receptor (Fig. 6c) with a consensus score of 63. Comparing both compounds with the inactive analog, harmine highlighted the retardation effect of methylated benzene of indole moiety. Furthermore, the potent unsubstituted derivative, harmane, showed HB with Gln:278A (Fig. 6d) with a consensus score of 56.

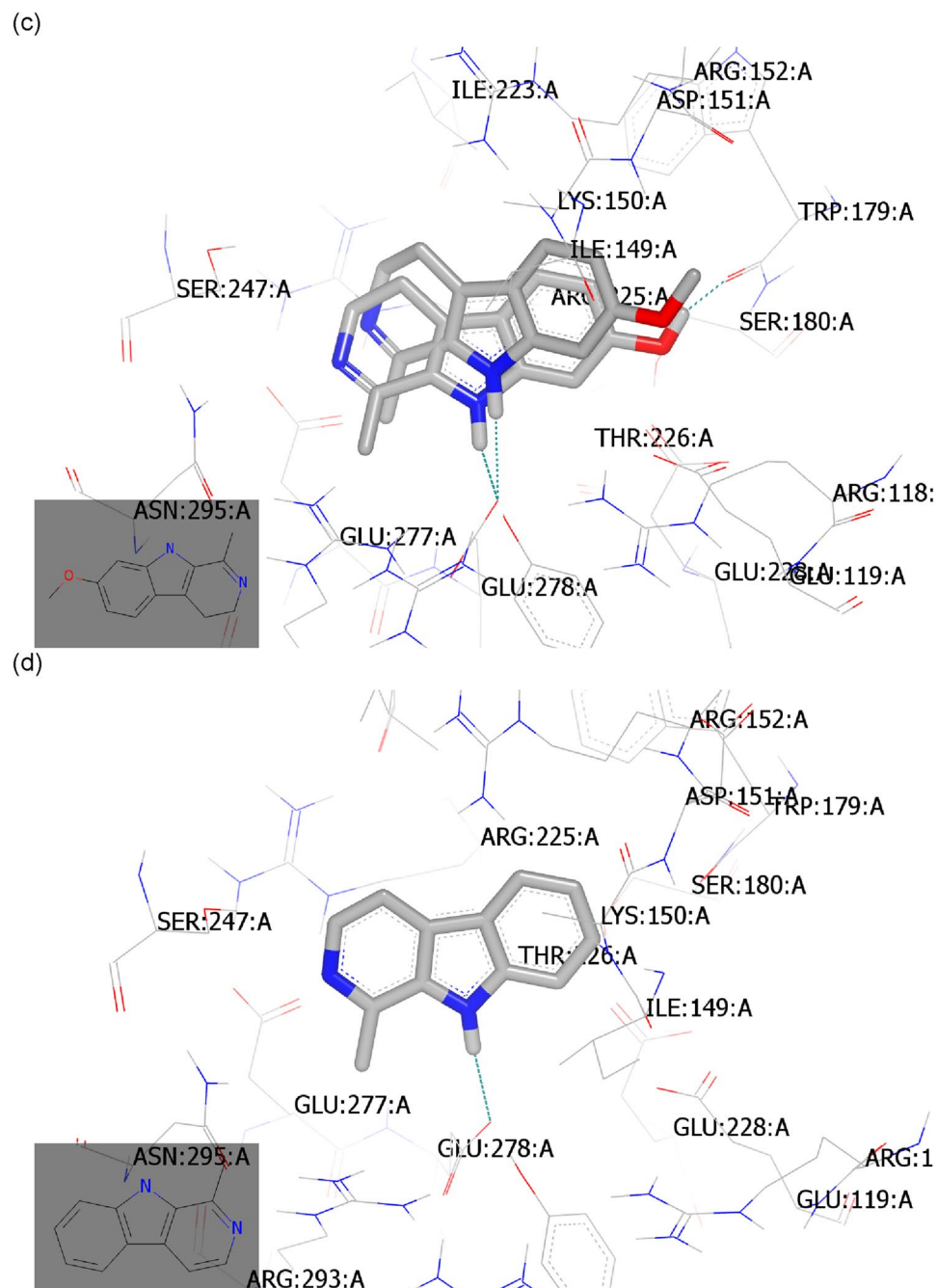


Figure 6. (continued)

Ligand efficiency and lipophilic efficiency profile⁵². Evaluating the lipophilicity profile in the ligand-target interaction concept is an important aspect of the druggability of new bioactive candidates. Presently, rationalization of both molecular size, and lipophilicity (cLogP) with drug activities (pIC_{50}) designated is essential. Ligand efficiency (LE) of bioactive compounds is assessed based on pIC_{50} in relation to the number of heavy atoms in a molecule known as non-hydrogen atoms (NHAs). LE estimates the affinity of drugs based on their size instead of considering the effectiveness or binding affinity of the whole structure. $\text{LE} = \Delta G \div \text{NHA}$ or $\text{LE} = (\text{pIC}_{50} \times 1.37) \div \text{NHA}$; where ΔG = Gibbs' free energy, IC_{50} = half-maximal inhibitory concentration (in terms of molar concentration), and NHA = non-hydrogen atom.

The challenge in the druggability of new drug candidates is in increasing the activity while keeping lipophilicity constant to avoid any “molecular obesity” during the drug development process. The other parameter of lipophilicity is the ligand lipophilic efficiency (LLE). LLE is a way to calculate the affinity of a drug candidate's function in its lipophilicity. LLE is the difference between the potency and ClogP according to the following equation: $\text{LLE} = \text{pIC}_{50} - \text{ClogP}$. Table 5 illustrated selected physicochemical properties which controlled the rule of five. All compounds have a small molecular weight in the range of 182–200. Both harmalol and harmaline displayed the same number of HB as acceptor (value 3) while harmane has HB as an acceptor of value 2. Both

Compound	Mwt	NHA	ClogP	PSA	Rotatable bond	Lipinski acceptor	Lipinski donor	PIC50 H5N1	LE	LEE	PIC50 H1N1	LE	LEE
Harmalol	200	15	0.97	48	0	3	2	7.677	0.70	6.71	7.70	0.70	6.73
Harmame	182	14	2.56	28	0	2	1	7.638	0.75	5.08	7.74	0.76	5.18
Harmaline	214	16	1.71	37	1	3	1	4.552	0.39	2.84	7.70	0.70	6.74

Table 5. Physicochemical parameters and lipophilicity metrics for selected carboline alkaloids. M.wt: Molecular Weight, NHA: non-hydrogen atom known as a number of heavy atoms, Clog P: lipophilicity, IC₅₀: Inhibitory Concentration, pIC₅₀: -log IC₅₀ (indicates drug potency), LE: Ligand efficiency, LLE: ligand lipophilic efficiency.

harmame and harmaline have the same HB as a donor (value 1) while harmalol has One HB as a donor. Only harmaline has one rotatable bond. The polar surface area for harmalol, harmaline, and harmame are 48, 37, and 28 respectively. The naturally occurring indole alkaloids in (Table 4) showed LE values against H1N1 and H5N1 of 0.69–0.75. The acceptable LE value should be more than 0.3. However, all compounds revealed LEE values in the range of 6.43–7.32. An LLE value ≥ 5 is recommended for drug candidates.

Structure–activity relationship (SAR). Generally, carboline alkaloids revealed better antiviral activities than indole alkaloids except strychnine sulfate showed potent in vitro activity against H1N1 (IC₅₀ = 0.06 $\mu\text{g/ml}$). Harmine and Norharmame have no effect. Harmalol, Harmame, and Harmaline illustrated equal activity against both viruses and were more potent than standard zanamivir drug. Furthermore, the free NH of the indole skeleton and low molecular weight seem important in compound activity. Among these alkaloids, harmalol has the highest PSA value and displayed the best lipophilicity metrics (LE and LEE). The compound's geometry and aromaticity illustrated the retardation effect in compound activity especially in the case of harmaline in comparison to the inactive compound harmine.

Discussion

Influenza is a highly transmissible respiratory disease that occasionally causes pandemics as well as seasonal epidemics. The annual seasonal viral epidemics kill up to 1 million people and infect about 10% of the human population all over the world⁵³. Despite that immunization is crucial and may help to minimize the viral infection severity, it only works when the vaccine matches the target viral strains that are already in circulation^{54–56}.

There are different FDA-approved and/or licensed anti-influenza agents available in the global markets, but their efficacy to control epidemic and pandemic influenza A viruses is now questionable with increased ratios of drug-resistant variants¹. The viral resistance against the available anti-influenza medications is the result of the development of IAV strains under the selection pressure of “antigenic shift” and/or “antigenic drift”^{1,57}. In this context, the decreased susceptibility to the already established antiviral medications urges the need to find new antiviral agents to combat the emerging and re-emerging flu strains.

A huge number of naturally derived, biologically active compounds containing the indole nucleus serve as therapeutics for many diseases such as cancer, diabetes, and viral and microbial diseases⁵⁸. Hence, we sought to examine the antiviral efficacy of some indole and β -carboline indole alkaloids against seasonal influenza A/H1N1 and highly pathogenic avian influenza A/H5N1 viruses. Intriguingly, the highly promising indole alkaloid, Strychnine Sulfate, proved its ability to combat the tested avian IAV by blocking mainly the adsorption of the virus to MDCK host cells, however no documented data available regarding the antiviral and/or anti-influenza activity of strychnine sulfate.

On the same hand, the β -carboline indole alkaloids including Harmalol and Harmaline showed highly promising anti-influenza activities against influenza A/H1N1 and A/H5N1 viruses. Previous results on the total seed extract of *Peganum harmala* L. containing Harmalol, Harmine, Harmaline, and Harmame proved to exert anti-influenza activity against influenza A/Puerto Rico/8/34 (H1N1; PR8) virus with an IC₅₀ value of 9.87 $\mu\text{g/ml}$ for the crude extract and 5.8 $\mu\text{g/ml}$ for the total purified alkaloids^{59,60}. However, rare or no information is available about the anti-influenza activities of Harmalol or Harmaline as purified compounds.

On the other hand, Harmame was shown to elucidate its capacity to counteract both seasonal human A/H1N1 virus and avian influenza A/H5N1 virus. In addition to the diverse range of Harmame, the purified Harmame from two different Simira plants, a genus of plants in the family Rubiaceae, showed antiviral potential against two different types of herpes simplex viruses (HSV-1 and HSV-2) with EC₅₀ (half maximal effective concentration) values of 4.90 $\mu\text{g/ml}$ for HSV-1 and 71.8 $\mu\text{g/ml}$ for HSV-2³⁵. Regarding the influenza viruses, no evident proof of the anti-influenza properties of pure Harmame was found in the literature. however *P. harmala* seeds extract undergone previous in vivo study against IAV⁶⁰.

As to their safety, strychnine is known to cause muscle contraction and convulsions that can lead to respiratory paralysis at high dose of 1.5 mg/kg⁶¹. In the same line, alkaloids from *P. harmala* seeds extract were reported to be toxic at higher doses ranging from 38 to 200 mg/kg in experimental animals⁶². This confirm that these studied alkaloids are highly tolerated in vivo due to previous studies, but they should be further confirmed in vivo to prove their safety and efficacy.

On the contrary, Reserpine was documented to have a robust antiviral activity against severe acute respiratory syndrome coronavirus (SARS-CoV) with an EC₅₀ value of 3.4 μM ¹⁵ whilst in our findings, it proved moderate anti-influenza potential against the human influenza A/H1N1 virus. Similarly, an in silico study for the antiviral activity of the Eserine (or Physostigmine) derivatives against pandemic SARS-CoV-2 proved their ability to combat the coronavirus action¹⁴. However, the purified compound of the Eserine used in this study

showed no antiviral activity against the human influenza A/H1N1 virus. Moreover, documented data regarding the antiviral activities of the β -carboline indole alkaloid, Harmine, proved its extensive use as an antiviral agent against HSV-2 with an EC₅₀ value of 1.47 μ M¹⁷. However, 9 N methylharmine, a Harmine derivative, proved to inhibit the DENV-2 (dengue virus-2) with an EC₅₀ value of 3.2 \pm 0.6 μ M¹⁸. Furthermore, Harmine exerted an antiviral property against EV-71 (Enterovirus-71) infection with an EC₅₀ value of and 20 μ M¹⁹. Nevertheless, our study proved no anti-influenza activity of the purified β -carboline indole alkaloid, Harmine, against avian influenza A/H5N1 virus.

Moreover, the four potent anti-influenza candidates can affect the viral replication cycle at multiple stages with variable inhibition levels, Strychnine Sulfate can predominately impair viral adsorption, while Harmalol and Harmine can affect mainly by interfering with the viral replication and finally Harmaline that affects the virus predominately in a cell-free status (direct virucidal effect). Nevertheless, this stage of the mechanism study is a preliminary overview to highlight the possible stage(s) in the viral replication cycle that may get affected during treatment with the investigated compound. To this point, further molecular investigations are demanded to specifically define the exact viral and cellular targets of the investigated compounds.

Conclusively, this study highlighted some alkaloids with robust anti-influenza activity. By applying the chemoinformatic studies, we found that harmalol displayed the best druggability parameters, especially LE and LLE) against both viruses. We, therefore, recommend that the antiviral activities of the studied effective alkaloids have to be widely studied including in vivo studies.

Conclusion

Alkaloids are natural secondary metabolites of plant origin that increasingly attract attention due to their numerous pharmacological actions including antiviral activities. This study could successfully investigate the anti-influenza efficacy of some distinct biologically active indole and β -carboline (β C) indole alkaloids against seasonal human-type IAV and avian-type IAV. Interestingly, β -carboline (β C) indole alkaloids displayed robust anti-influenza activities against the predefined strains via multiple modes of action. Cheminformatics studies and lipophilicity metrics for active compounds illuminate our direction for further studies for preclinical and clinical phases as antiviral drug candidates.

Data availability

All data generated or analyzed during this study are included in this published article.

Received: 13 September 2022; Accepted: 10 January 2023

Published online: 28 January 2023

References

- Mostafa, A., Abdelwhab, E. M., Mettenleiter, T. C. & Pleschka, S. Zoonotic potential of influenza A viruses: A comprehensive overview. *Viruses* **10**, 497. <https://doi.org/10.3390/v10090497> (2018).
- Short, K. R., Kedzierska, K. & Van de Sandt, C. E. Back to the future: Lessons learned from the 1918 influenza pandemic. *Front. Cell. Infect. Microbiol.* **8**, 343 (2018).
- Kilbourne, E. D. Influenza pandemics of the 20th century. *Emerg. Infect. Dis.* **12**, 9 (2006).
- Monto, A. S. & Fukuda, K. Lessons from influenza pandemics of the last 100 years. *Clin. Infect. Dis.* **70**, 951–957 (2020).
- Ti, H., Zhuang, Z., Yu, Q. & Wang, S. Progress of plant medicine derived extracts and alkaloids on modulating viral infections and inflammation. *Drug Des. Dev. Ther.* **15**, 1385 (2021).
- Abookleesh, F. L., Al-Anzi, B. S. & Ullah, A. Potential antiviral action of alkaloids. *Molecules* **27**, 903 (2022).
- Ain, Q.-U., Khan, H., Mubarak, M. S. & Pervaiz, A. Plant alkaloids as antiplatelet agent: Drugs of the future in the light of recent developments. *Front. Pharmacol.* **7**, 292 (2016).
- Dey, P. *et al.* Analysis of alkaloids (indole alkaloids, isoquinoline alkaloids, tropane alkaloids). *Recent Adv. Nat. Prod. Anal.* **2020**, 505–67. <https://doi.org/10.1016/B978-0-12-816455-6.00015-9> (2020).
- Kadam, R. U. & Wilson, I. A. Structural basis of influenza virus fusion inhibition by the antiviral drug Arbidol. *Proc. Natl. Acad. Sci.* **114**, 206–214 (2017).
- Devogelaere, B. *et al.* TMC647055, a potent nonnucleoside hepatitis C virus NS5B polymerase inhibitor with cross-genotypic coverage. *Antimicrob. Agents Chemother.* **56**, 4676–4684 (2012).
- Ruiz, F. X., Hoang, A., Das, K. & Arnold, E. Structural basis of HIV-1 inhibition by nucleotide-competing reverse transcriptase inhibitor INDOPY-1. *J. Med. Chem.* **62**, 9996–10002. <https://doi.org/10.1021/acs.jmedchem.9b01289> (2019).
- Monsalve-Escudero, L. M. *et al.* The antiviral and virucidal activities of voacangine and structural analogs extracted from *tabernaemontana cymosa* depend on the dengue virus strain. *Plants* **10**, 1280 (2021).
- Monsalve-Escudero, L. M. *et al.* Indole alkaloids inhibit zika and chikungunya virus infection in different cell lines. *BMC Complement. Med. Ther.* **21**, 1–17 (2021).
- Llanes, A., Cruz, H., Nguyen, V. D., Larionov, O. V. & Fernandez, P. L. A. Computational approach to explore the interaction of semisynthetic nitrogenous heterocyclic compounds with the SARS-CoV-2 main protease. *Biomolecules* **11**, 18. <https://doi.org/10.3390/biom11010018> (2020).
- Khan, T., Khan, M. A., Mashwani, Z. U., Ullah, N. & Nadhman, A. Therapeutic potential of medicinal plants against COVID-19: The role of antiviral medicinal metabolites. *Biocatal. Agric. Biotechnol.* **31**, 101890. <https://doi.org/10.1016/j.bcab.2020.101890> (2021).
- Fayed, M. A. A. *et al.* Structure- and ligand-based in silico studies towards the repurposing of marine bioactive compounds to target SARS-CoV-2. *Arab. J. Chem.* **14**, 103092. <https://doi.org/10.1016/j.arabjc.2021.103092> (2021).
- Chen, D. *et al.* Harmine blocks herpes simplex virus infection through downregulating cellular NF-kappaB and MAPK pathways induced by oxidative stress. *Antivir. Res.* **123**, 27–38. <https://doi.org/10.1016/j.antiviral.2015.09.003> (2015).
- Quintana, V. M. *et al.* Antiviral activity of natural and synthetic beta-carbolines against dengue virus. *Antivir. Res.* **134**, 26–33. <https://doi.org/10.1016/j.antiviral.2016.08.018> (2016).
- Chen, D. *et al.* Harmine, a small molecule derived from natural sources, inhibits enterovirus 71 replication by targeting NF- κ B pathway. *Int. Immunopharmacol.* **60**, 111–120 (2018).
- Ding, Y. *et al.* Harmine induces anticancer activity in breast cancer cells via targeting TAZ. *Int. J. Oncol.* **54**, 1995–2004. <https://doi.org/10.3892/ijo.2019.4777> (2019).

21. Asgarpanah, J. & Ramezanloo, F. Chemistry, pharmacology and medicinal properties of *Peganum harmala* L.. *Afr. J. Pharm. Pharmacol* **6**, 1573–1580 (2012).
22. Mostafa, A. *et al.* PA from a recent H9N2 (G1-Like) avian influenza A virus (AIV) strain carrying lysine 367 confers altered replication efficiency and pathogenicity to contemporaneous H5N1 in mammalian systems. *Viruses* **12**, 1046. <https://doi.org/10.3390/v12091046> (2020).
23. Petersen, H. *et al.* NS segment of a 1918 influenza A virus-descendant enhances replication of H1N1pdm09 and virus-induced cellular immune response in mammalian and avian systems. *Front. Microbiol.* **9**, 526 (2018).
24. Rao, P. S., Ramanadham, M. & Prasad, M. N. Anti-proliferative and cytotoxic effects of strychnos nux-vomica root extract on human multiple myeloma cell line—RPMI 8226. *Food Chem. Toxicol.* **47**, 283–288. <https://doi.org/10.1016/j.fct.2008.10.027> (2009).
25. Skurikhin, E. G. *et al.* Mechanisms of the anti-inflammatory and antifibrotic activity of a sympatholytic agent during toxic pulmonary fibrosis. *Bull. Exp. Biol. Med.* **153**, 638–643. <https://doi.org/10.1007/s10517-012-1786-5> (2012).
26. Shamon, S. D. & Perez, M. I. Blood pressure-lowering efficacy of reserpine for primary hypertension. *Cochrane Database Syst. Rev.* **12**, CD007655. <https://doi.org/10.1002/14651858.CD007655.pub3> (2016).
27. Li, M., Li, P., Zhang, M. & Ma, F. Brucine suppresses breast cancer metastasis via inhibiting epithelial mesenchymal transition and matrix metalloproteinases expressions. *Chin. J. Integr. Med.* **24**, 40–46. <https://doi.org/10.1007/s11655-017-2805-1> (2018).
28. Lu, L. *et al.* Brucine: A review of phytochemistry, pharmacology, and toxicology. *Front. Pharmacol.* **11**, 377. <https://doi.org/10.3389/fphar.2020.00377> (2020).
29. Omar, F. *et al.* Plant-based indole alkaloids: A comprehensive overview from a pharmacological perspective. *Molecules* **26**, 2297. <https://doi.org/10.3390/molecules26082297> (2021).
30. Gallos, I. D. *et al.* Uterotonic agents for preventing postpartum haemorrhage: a network meta-analysis. *Cochrane Database Syst. Rev.* **12**, CD011689. <https://doi.org/10.1002/14651858.CD011689.pub3> (2018).
31. Kim, Y. H. *et al.* Reduced neuronal proliferation by proconvulsant drugs in the developing zebrafish brain. *Neurotoxicol. Teratol.* **32**, 551–557. <https://doi.org/10.1016/j.ntt.2010.04.054> (2010).
32. Olmedo, G. M. *et al.* Antifungal activity of β -carboline on *Penicillium digitatum* and *Botrytis cinerea*. *Food Microbiol.* **62**, 9–14 (2017).
33. El Gendy, M. A., Soshilov, A. A., Denison, M. S. & El-Kadi, A. O. Harmaline and harmalol inhibit the carcinogen-activating enzyme CYP1A1 via transcriptional and posttranslational mechanisms. *Food Chem. Toxicol.* **50**, 353–362 (2012).
34. Khan, H., Patel, S. & Kamal, A. M. Pharmacological and toxicological profile of harmaline- β -carboline alkaloid: Friend or foe. *Curr. Drug Metabol.* **18**, 853–857 (2017).
35. Cavalcanti, J. F. *et al.* Proposed anti-HSV compounds isolated from simira species. *Nat. Prod. Res.* **32**, 2720–2723 (2018).
36. Gonzalez, M. M. *et al.* β -Carboline derivatives as novel antivirals for herpes simplex virus. *Int. J. Antimicrob. Agents* **52**, 459–468 (2018).
37. Herraiz, T. & Guillén, H. Monoamine oxidase—A inhibition and associated antioxidant activity in plant extracts with potential antidepressant actions. *BioMed Res. Int.* **2018**, 4810394 (2018).
38. Roy, S. *et al.* Discovery of harmaline as a potent inhibitor of sphingosine kinase-1: A chemopreventive role in lung cancer. *ACS Omega* **5**, 21550–21560 (2020).
39. Sahoo, C. R., Paidasetty, S. K. & Padhy, R. N. Norharmaline as a potential chemical entity for development of anticancer drugs. *Eur. J. Med. Chem.* **162**, 752–764 (2019).
40. Lee, J.-H., Kim, Y.-G., Shim, S. H. & Lee, J. Antibiofilm activities of norharmaline and its derivatives against *Escherichia coli* O157: H7 and other bacteria. *Phytomedicine* **36**, 254–261 (2017).
41. Reed, L. J. & Muench, H. A simple method of estimating fifty per cent endpoints. *Am. J. Epidemiol.* **27**, 493–497 (1938).
42. Gaush, C. R. & Smith, T. F. Replication and plaque assay of influenza virus in an established line of canine kidney cells. *Appl. Microbiol.* **16**, 588–594 (1968).
43. Mahmoud, A. *et al.* Telaprevir is a potential drug for repurposing against SARS-CoV-2: Computational and in vitro studies. *Heliyon* **7**, e07962 (2021).
44. Mostafa, A. *et al.* FDA-approved drugs with potent in vitro antiviral activity against severe acute respiratory syndrome coronavirus 2. *Pharmaceuticals* **13**, 443. <https://doi.org/10.3390/ph13120443> (2020).
45. Feoktistova, M., Geserick, P. & Leverkus, M. Crystal violet assay for determining viability of cultured cells. *Cold Spring Harb. Protoc.* **2016**, pdb.prot087379. <https://doi.org/10.1101/pdb.prot087379> (2016).
46. Zima, V. *et al.* Investigation of flexibility of neuraminidase 150-loop using tamiflu derivatives in influenza A viruses H1N1 and H5N1. *Bioorg. Med. Chem.* **27**, 2935–2947. <https://doi.org/10.1016/j.bmc.2019.05.024> (2019).
47. Thomaston, J. L. *et al.* Inhibitors of the M2 proton channel engage and disrupt transmembrane networks of hydrogen-bonded waters. *J. Am. Chem. Soc.* **140**, 15219–15226. <https://doi.org/10.1021/jacs.8b06741> (2018).
48. Hegazy, A. *et al.* Robust antiviral activity of santonica flower extract (*Artemisia cina*) against avian and human influenza A viruses: In vitro and chemoinformatic studies. *ACS Omega* <https://doi.org/10.1021/acsomega.2c04867> (2022).
49. Kausar, S. *et al.* A review: Mechanism of action of antiviral drugs. *Int. J. Immunopathol. Pharmacol.* **35**, 20587384211002620. <https://doi.org/10.1177/20587384211002621> (2021).
50. Kim, C. U. *et al.* Structure–activity relationship studies of novel carbocyclic influenza neuraminidase inhibitors. *J. Med. Chem.* **41**, 2451–2460. <https://doi.org/10.1021/jm980162u> (1998).
51. Berman, H., Henrick, K. & Nakamura, H. Announcing the worldwide protein data bank. *Nat. Struct. Biol.* **10**, 980. <https://doi.org/10.1038/nsb1203-980> (2003).
52. Hongmao, S. In *A practical guide to rational drug design* (ed. Hongmao, Sun) 163–192 (Woodhead Publishing, 2016).
53. Torabian, G., Valtchev, P., Adil, Q. & Dehghani, F. Anti-influenza activity of elderberry (*Sambucus nigra*). *J. Funct. Foods* **54**, 353–360 (2019).
54. Ulyanova, V. *et al.* Anti-influenza activity of the ribonuclease binase: Cellular targets detected by quantitative proteomics. *Int. J. Mol. Sci.* **21**, 8294 (2020).
55. Mostafa, A. & Pleschka, S. Influenza H3N2 vaccines: Recent challenges. *Trends Microbiol.* **26**, 87–89. <https://doi.org/10.1016/j.tim.2017.12.003> (2018).
56. Mostafa, A. *et al.* Phylogenetic analysis of human influenza A/H3N2 viruses isolated in 2015 in Germany indicates significant genetic divergence from vaccine strains. *Adv. Virol.* **161**, 1505–1515. <https://doi.org/10.1007/s00705-016-2815-x> (2016).
57. Liu, S.-S. *et al.* Susceptibility of influenza A (H1N1)/pdm2009, seasonal A (H3N2) and B viruses to Oseltamivir in Guangdong, China between 2009 and 2014. *Sci. Rep.* **7**, 1–11 (2017).
58. Omar, F. *et al.* Plant-based indole alkaloids: A comprehensive overview from a pharmacological perspective. *Molecules* **26**, 2297 (2021).
59. Moradi, M.-T., Karimi, A., Rafeian-Kopaei, M. & Fotouhi, F. In vitro antiviral effects of *Peganum harmala* seed extract and its total alkaloids against influenza virus. *Microb. Pathog.* **110**, 42–49 (2017).
60. Moradi, M. T., Karimi, A., Fotouhi, F., Kheiri, S. & Torabi, A. In vitro and in vivo effects of *Peganum harmala* L. seeds extract against influenza A virus. *Avicenna J. Phytomed.* **7**, 519–530 (2017).
61. Otter, J. & D’Orazio, J. L. *StatPearls* (StatPearls Publishing, 2022).
62. Moloudizargari, M., Mikaili, P., Aghajanshakeri, S., Asghari, M. H. & Shayegh, J. Pharmacological and therapeutic effects of *Peganum harmala* and its main alkaloids. *Pharmacogn. Rev.* **7**, 199–212. <https://doi.org/10.4103/0973-7847.120524> (2013).

Author contributions

Conceptualization, A.M.E., I.M. and A.M.; methodology, A.H., I.M., S.H.M., Y.A.M.M.E., N.M.A., N.F.N, M.A.A., and A.M.; formal analysis, A.H., M.A.A., A.M.E., I.M., A.M.; investigation, A.H., M.A.A., A.M.E., and A.M.; data curation, A.M. and M.A.A.; Supervision, M.A.A., N.F.N., and A.M.; writing—original draft preparation, A.H., I.M., and A.M.; writing—review and editing, all authors read and approved the final manuscript.

Funding

Open access funding provided by The Science, Technology & Innovation Funding Authority (STDF) in cooperation with The Egyptian Knowledge Bank (EKB). This research was funded by Egyptian National Research Centre (NRC)-funded projects (TT110801 and 12010126 to AM). The funders had no role in study design, data collection, and analysis, decision to publish, or preparation of the manuscript.

Competing interests

The authors declare no competing interests.

Additional information

Correspondence and requests for materials should be addressed to I.M. or A.M.

Reprints and permissions information is available at www.nature.com/reprints.

Publisher's note Springer Nature remains neutral with regard to jurisdictional claims in published maps and institutional affiliations.



Open Access This article is licensed under a Creative Commons Attribution 4.0 International License, which permits use, sharing, adaptation, distribution and reproduction in any medium or format, as long as you give appropriate credit to the original author(s) and the source, provide a link to the Creative Commons licence, and indicate if changes were made. The images or other third party material in this article are included in the article's Creative Commons licence, unless indicated otherwise in a credit line to the material. If material is not included in the article's Creative Commons licence and your intended use is not permitted by statutory regulation or exceeds the permitted use, you will need to obtain permission directly from the copyright holder. To view a copy of this licence, visit <http://creativecommons.org/licenses/by/4.0/>.

© The Author(s) 2023